Supplemental Info "Observing Low Altitude Features in Ozone Concentrations in a Shoreline Environment via Uncrewed Aerial Systems"

Josie K. Radtke[1], Benjamin N. Kies[1], Whitney A. Mottishaw[1], Sydney M. Zeuli[1], Aidan T.H. Voon[1], Kelly L. Koerber[1], Grant W. Petty[2], Michael P. Vermeuel[3†], Timothy H. Bertram[3], Ankur R. Desai[2], Joseph P. Hupy[4], R. Bradley Pierce[2,5], Timothy J. Wagner[5], Patricia A. Cleary[1]

Figure S1. Typhoon H UAS with mounted POM and iMet-XQ2 as flown during CHEESEHEAD-19 in 2019. POM was housed in foam for vibration dampening.

Figure S2. Top mounted iMet-XQ2 and POM on a DJI M600. The inlet to the POM is held up with a bracket to hold the inlet filter assembly (blue and white).

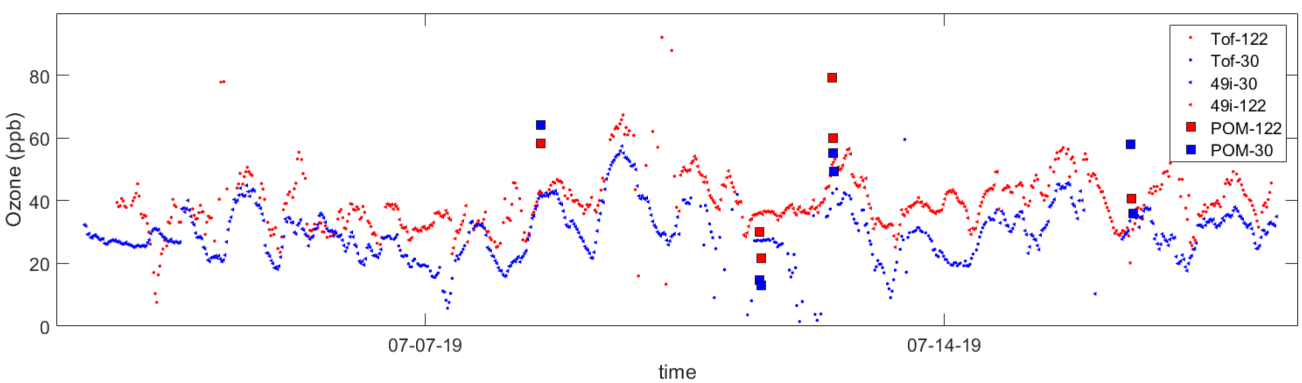

Figure S3: Tower ozone observations from Park Falls WLEF tower at 30 m (blue) and 120 m (red) using TOF and 49i photometric analyzer and UAS platform POM observations (squares) at same altitudes.

Section S1. Evidence of Lake Breeze

Satellite imagery, near-surface meteorology and Doppler lidar observations can be used to identify the presence of marine-influenced air during these field operations. Satellite imagery which shows a distinct lack of cumulous clouds over Lake Michigan with a clear delineation of a cumulous cloud front over land is evidence for a lake breeze, as seen in Figures S7-S10. Figures S12-S16 show the meteorology for the specific days of June 15-19, 2020. Note that the wind direction at the ground station changed from SW to SE most mornings this week, temperatures were rising before the wind shift and then plateaued or rose slower throughout the day after the wind direction change with the onset of the lake breeze.(Cleary et al., 2022),(Wagner et al., 2022) Surface meteorological observations show sustained wind shifts to E, SE or SSE at 10:40 UTC (5:40 CDT) on June 15, 11:20 UTC (6:20 CDT) on June 16, 10:40 UTC (5:40 CDT) on June 17, 13:20 UTC (8:20 CDT) on June 18 and 11:15 UTC (6:15 CDT) on June 19, 2020 (Figures S12-16). The corresponding lidar observations show easterly winds (negative *u* (zonal) winds) after the ground observation of a wind shift. The time of lake breeze onset discerned from the Doppler lidar data appears later than ground observations, after 14:00 UTC, 9:00 CDT on June 18 and 19, likely because recovery only starts at altitudes above 100 m AGL. Afternoon easterly winds extend to altitudes up to 1500-1000 m AGL on June 18 (Fig. S18b) and to 700 m AGL on June 19 (Fig. S19 b). The mid-afternoon marine layer, which we assign as altitudes with negative *u* (zonal) winds, showed multiple bands of higher backscatter on both June 18 (Fig. S18c) at 150 and 250 m AGL and June 19 (Fig. S19c.) at 500, 250 and 125 m AGL. High backscatter is attributed on these days to high particle concentrations in the atmosphere (where no fog was present).

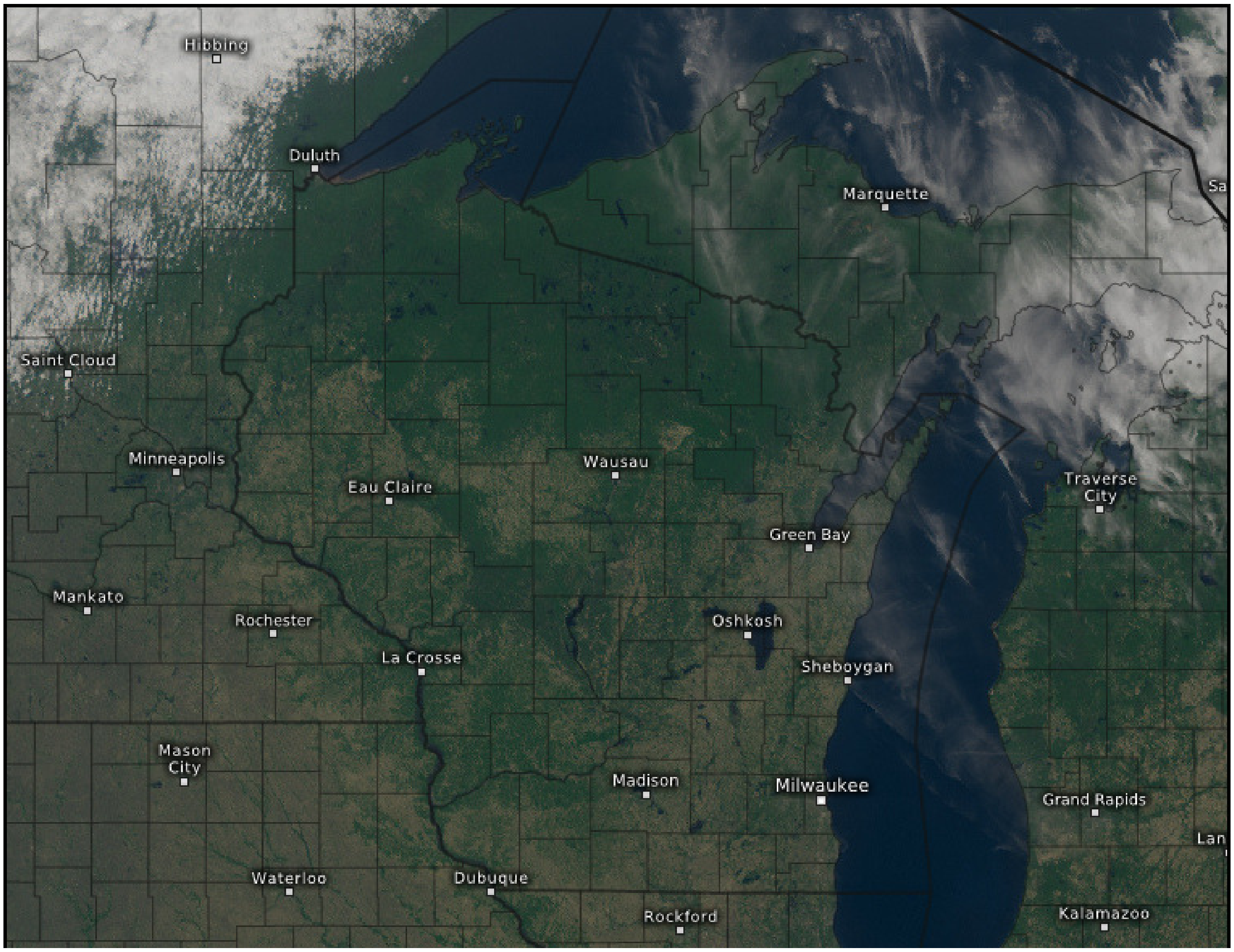

Figure S4: June 8, 2020 high definition color GOES-East satellite image of clouds over Wisconsin at 1400 CDT with a resolution of 1.0 km.

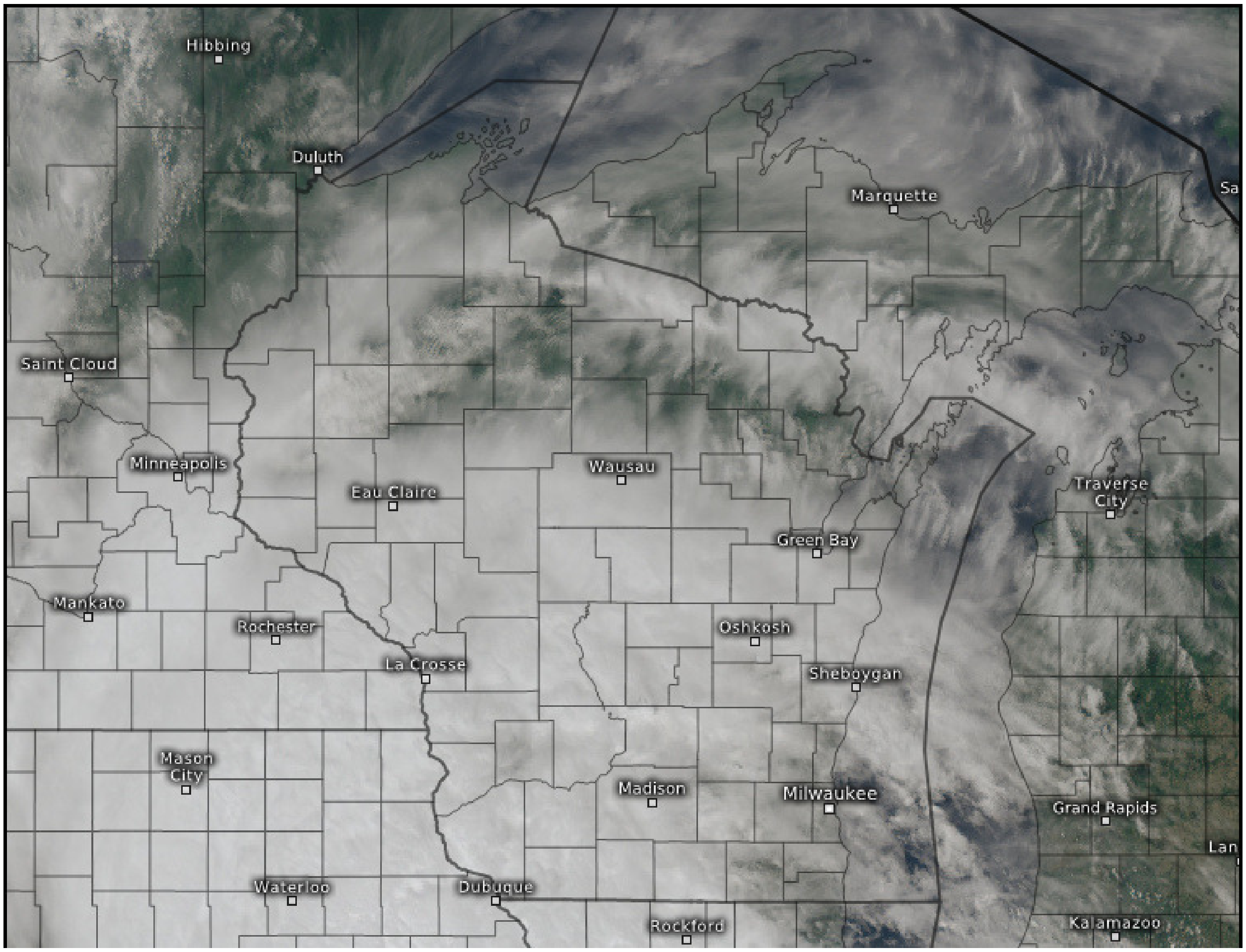

Figure S5: June 9, 2020 high definition color GOES-East satellite image of clouds over Wisconsin at 1400 CDT with a resolution of 1.0 km.

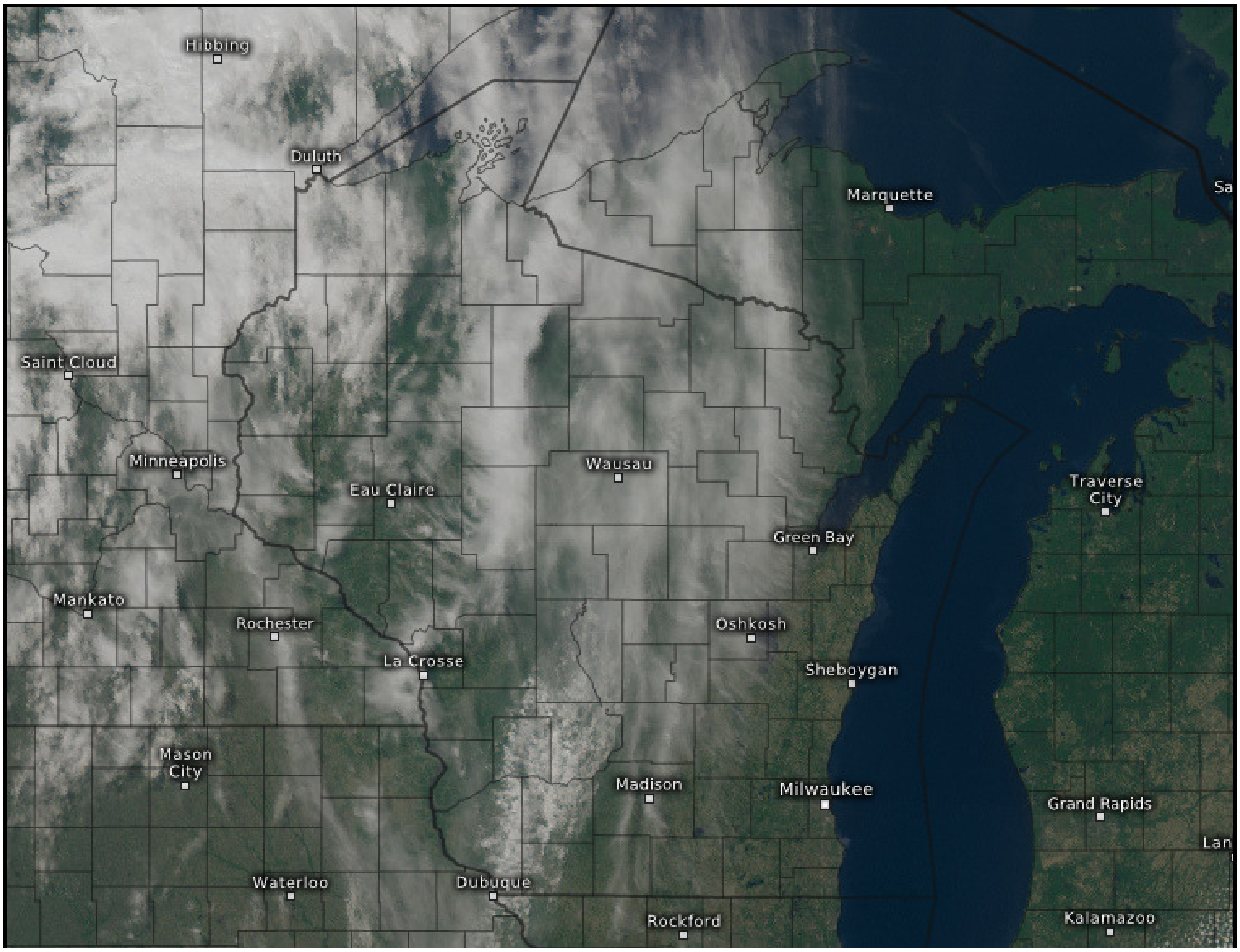

Figure S6: June 15, 2020 high definition color GOES-East satellite image of clouds over Wisconsin at 1400 CDT with a resolution of 1.0 km.

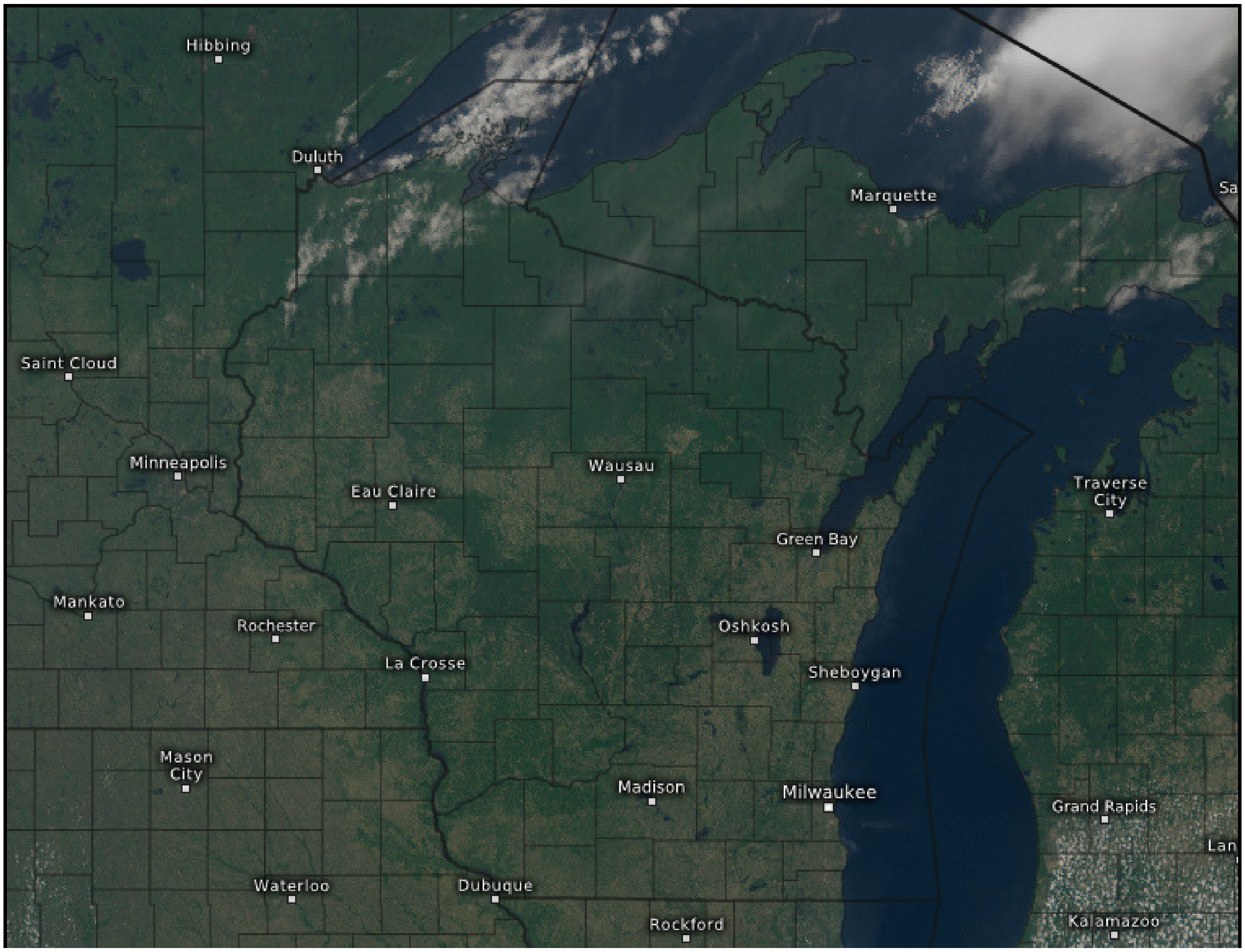

Figure S7: June 16, 2020 high definition color GOES-East satellite image of clouds over Wisconsin at 1400 CDT with a resolution of 1.0 km.

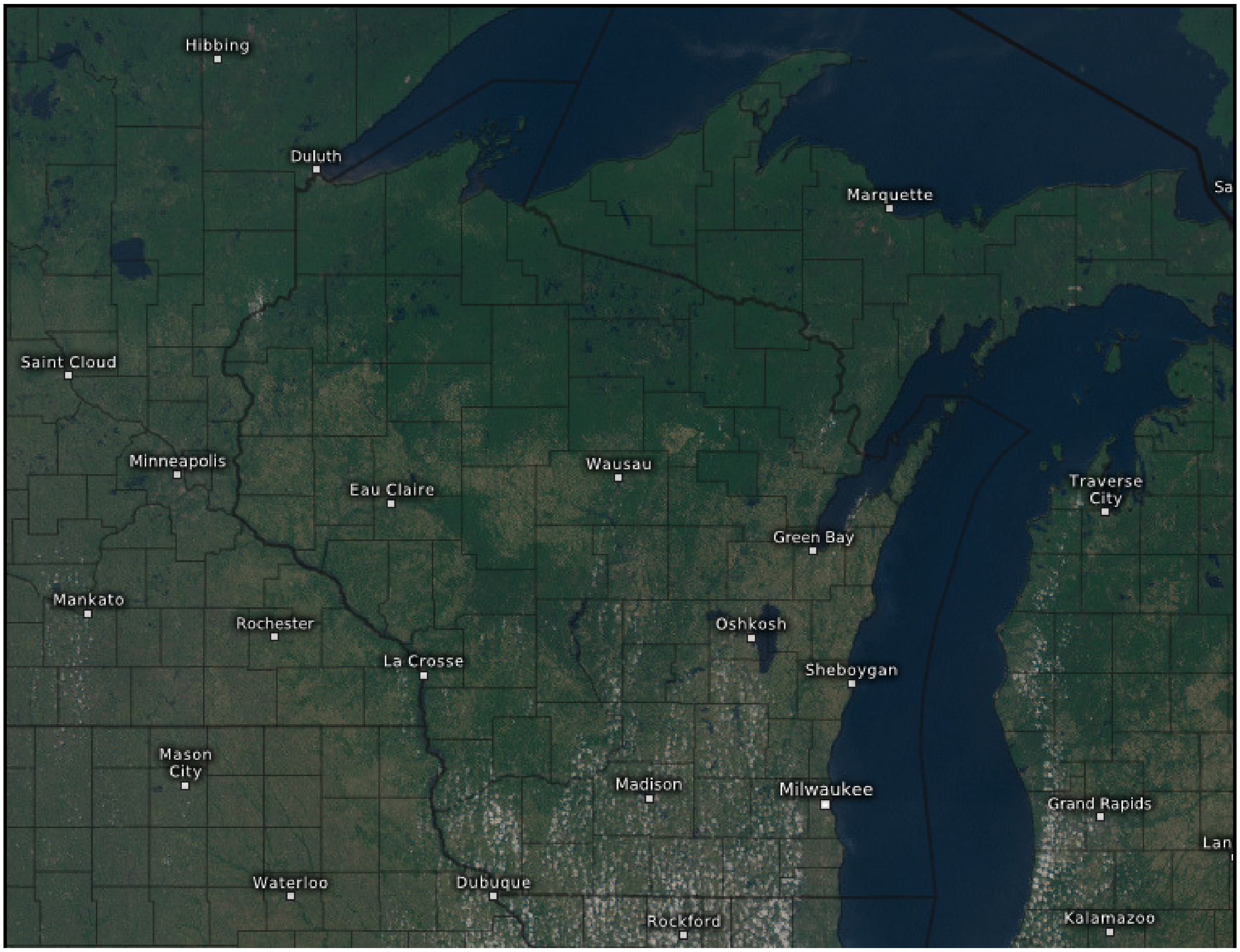

Figure S8: June 17, 2020 high definition color GOES-East satellite image of clouds over Wisconsin at 1400 CDT with a resolution of 1.0 km.

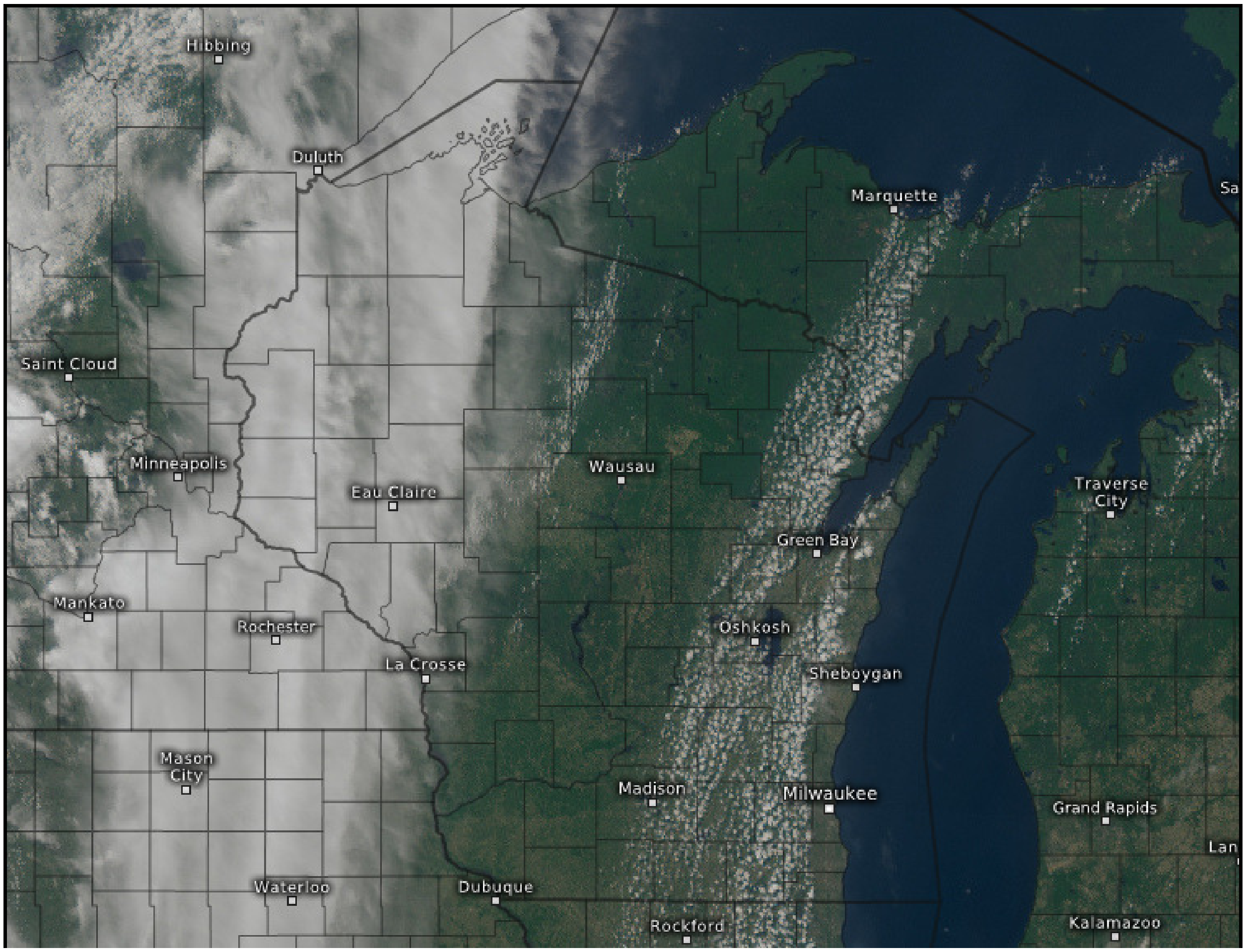

Figure S9: June 18, 2020 high definition color GOES-East satellite image of clouds over Wisconsin at 1400 CDT with a resolution of 1.0 km.

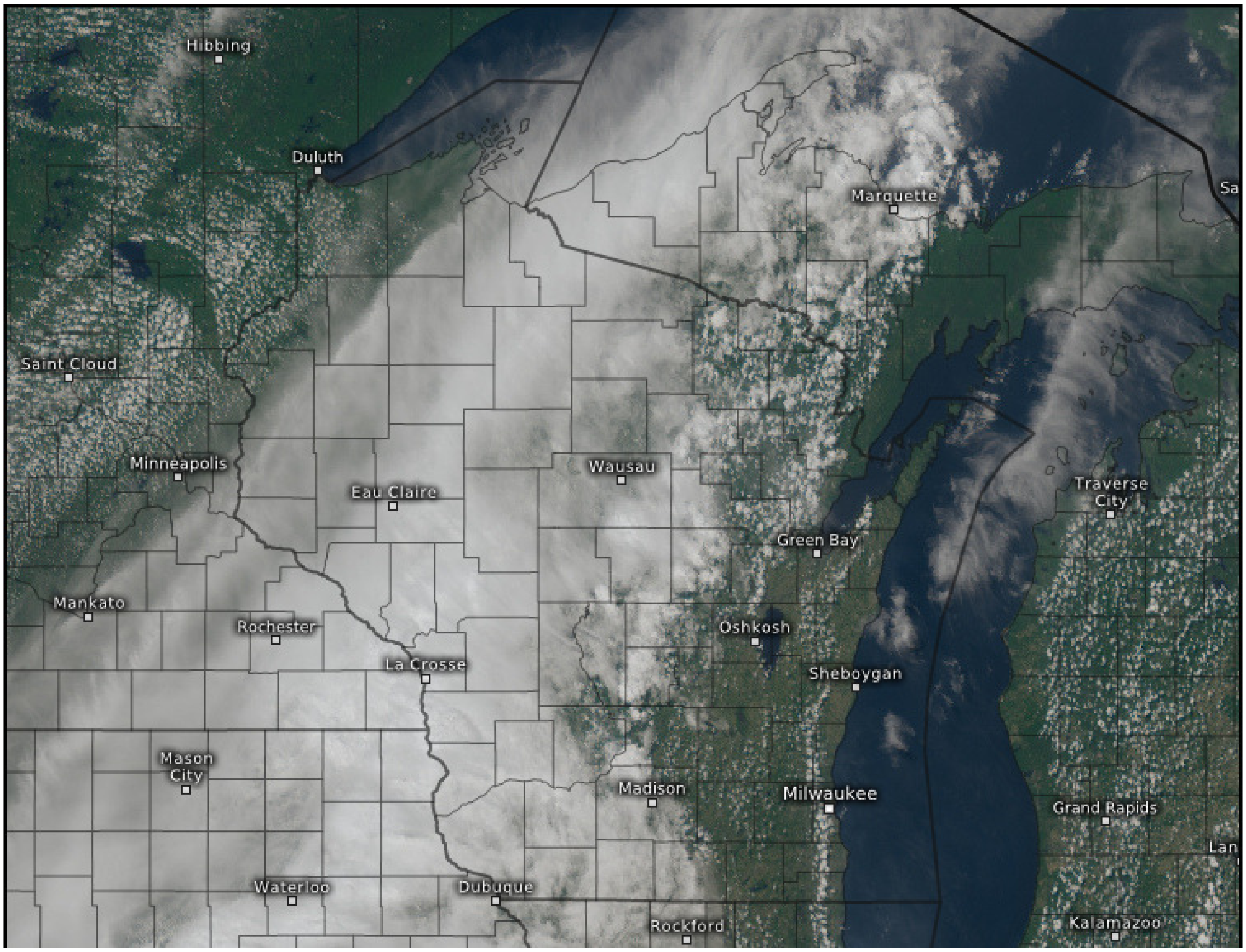

Figure S10: June 19, 2020 high definition color GOES-East satellite image of clouds over Wisconsin at 1400 CDT with a resolution of 1.0 km.

Figure S11: WISCODisco20 field work image at Chiwaukee Prairie State Natural Area. The right side of this image shows cloud suppression over Lake Michigan during this field campaign.

S2. Meteorology June 15-19, 2020

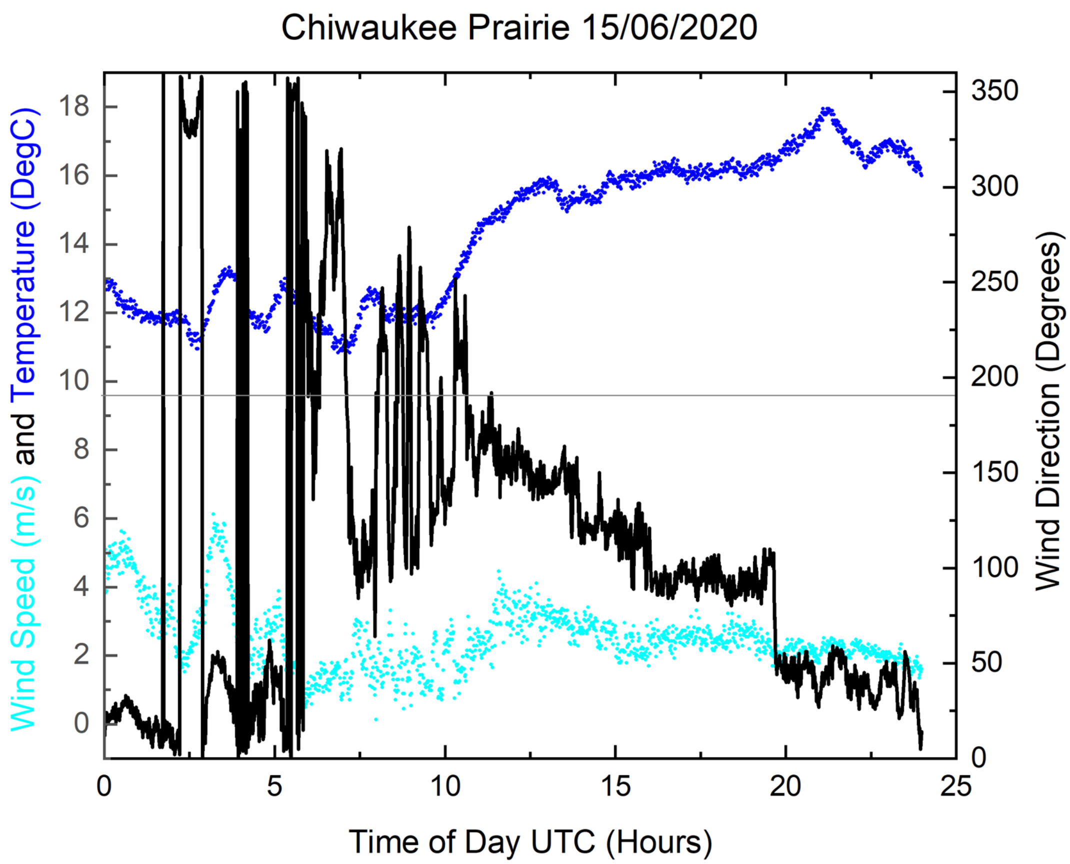

Figure S12: Ground station meteorological observations of wind speed (m/s), direction and air temperature (in ^{o} C) at Chiwaukee Prairie on June 15, 2020

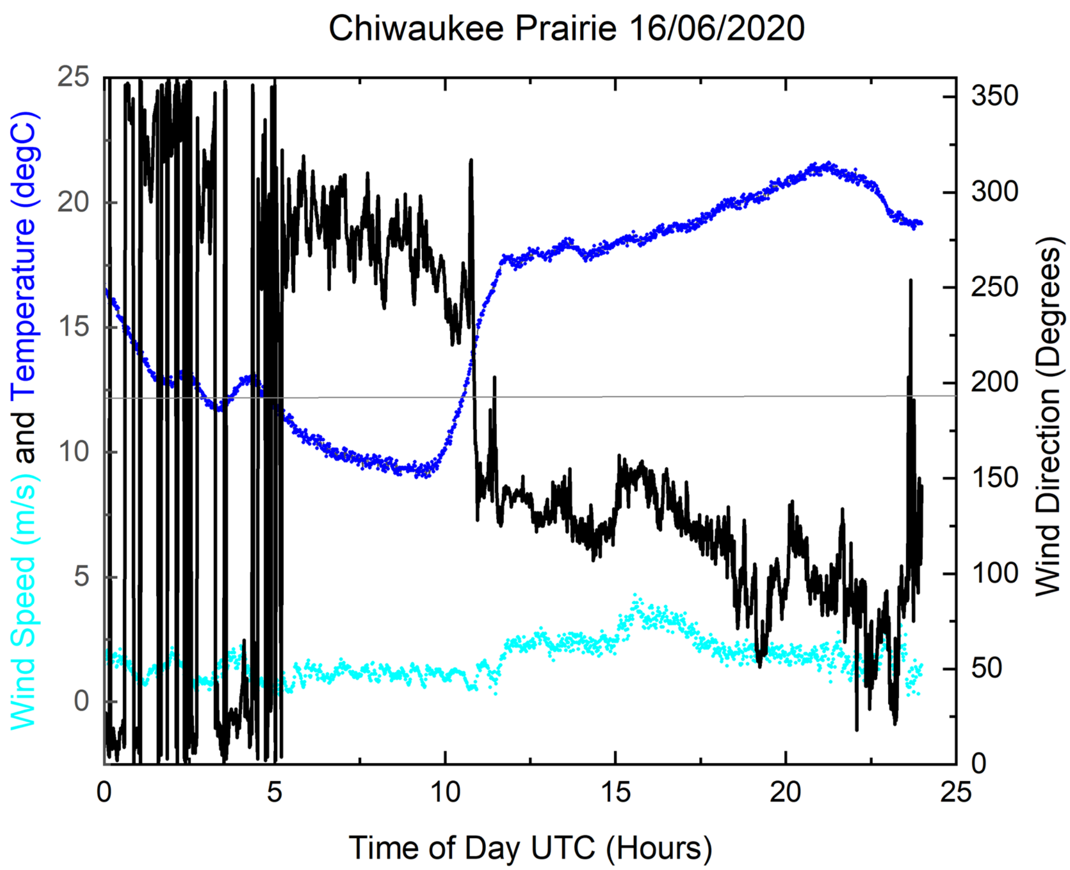

Figure S13: Ground station meteorological observations of wind speed (m/s), direction and air temperature (in ^{o} C) at Chiwaukee Prairie on June 16, 2020

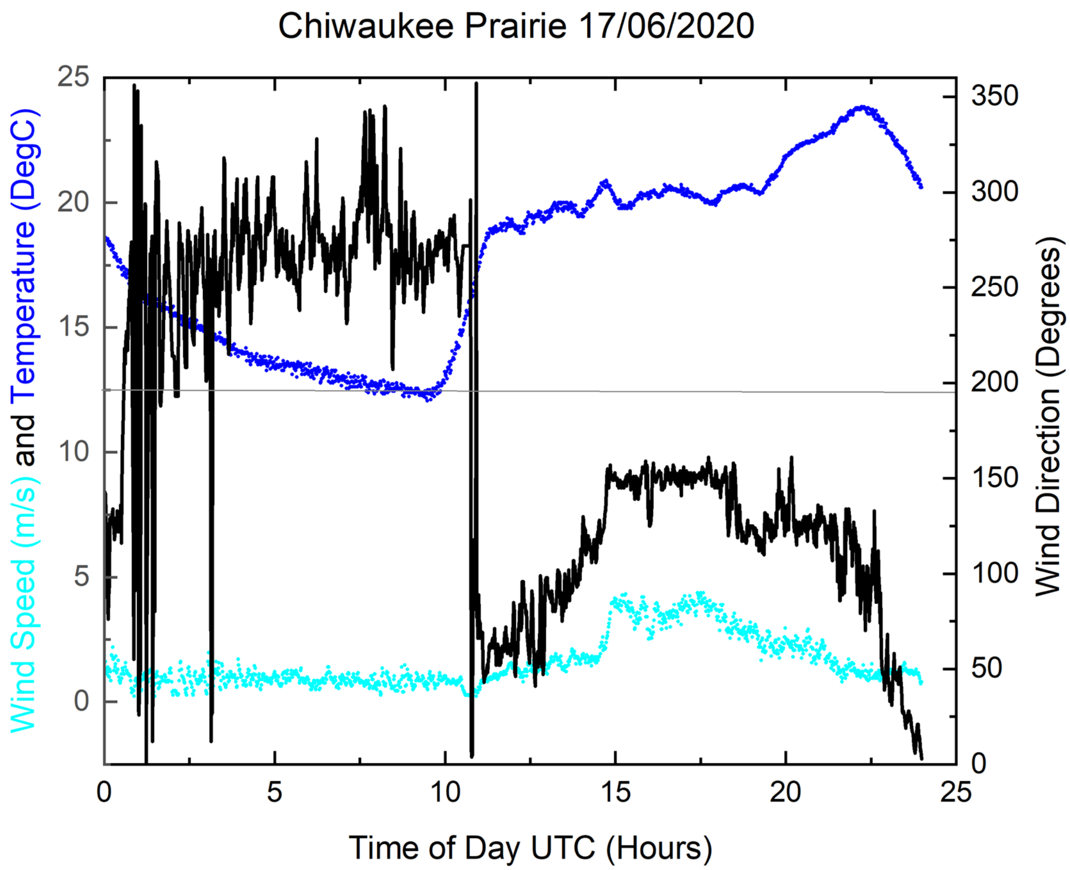

Figure S14: Ground station meteorological observations of wind speed (m/s), direction and air temperature (in ^{o} C) at Chiwaukee Prairie on June 17, 2020

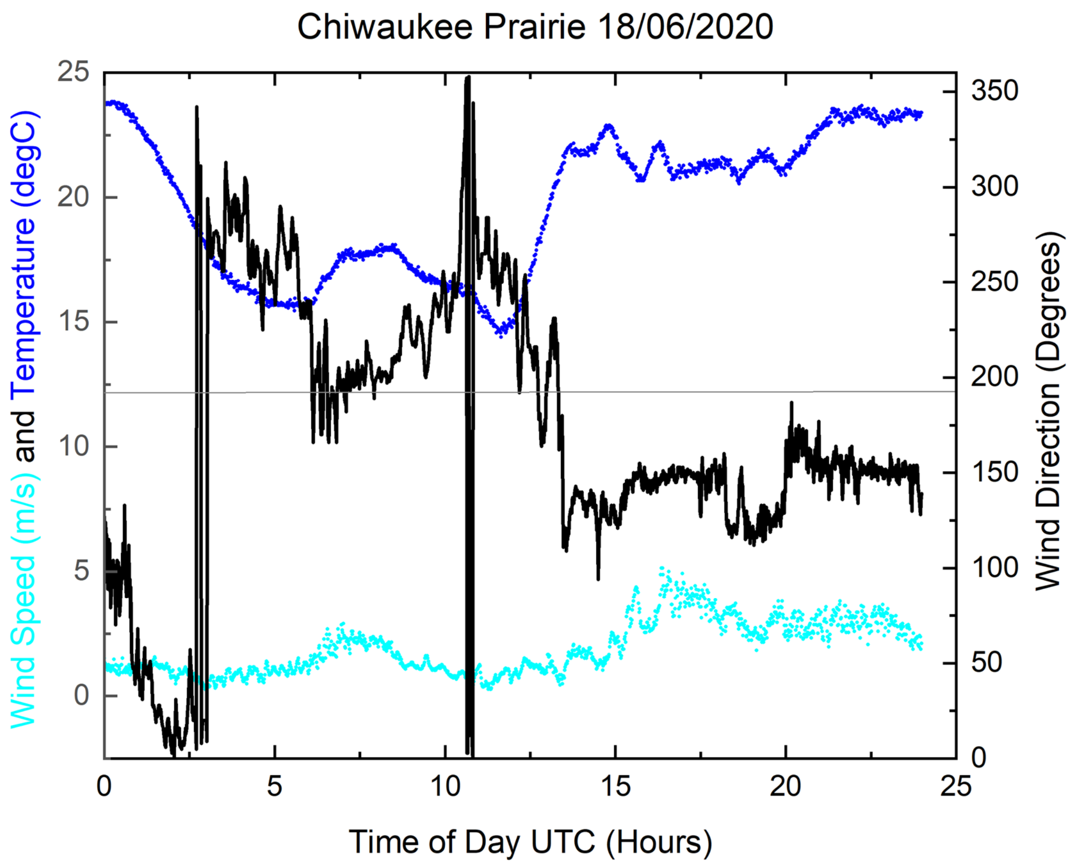

Figure S15: Ground station meteorological observations of wind speed (m/s), direction and air temperature (in ^{o} C) at Chiwaukee Prairie on June 18, 2020

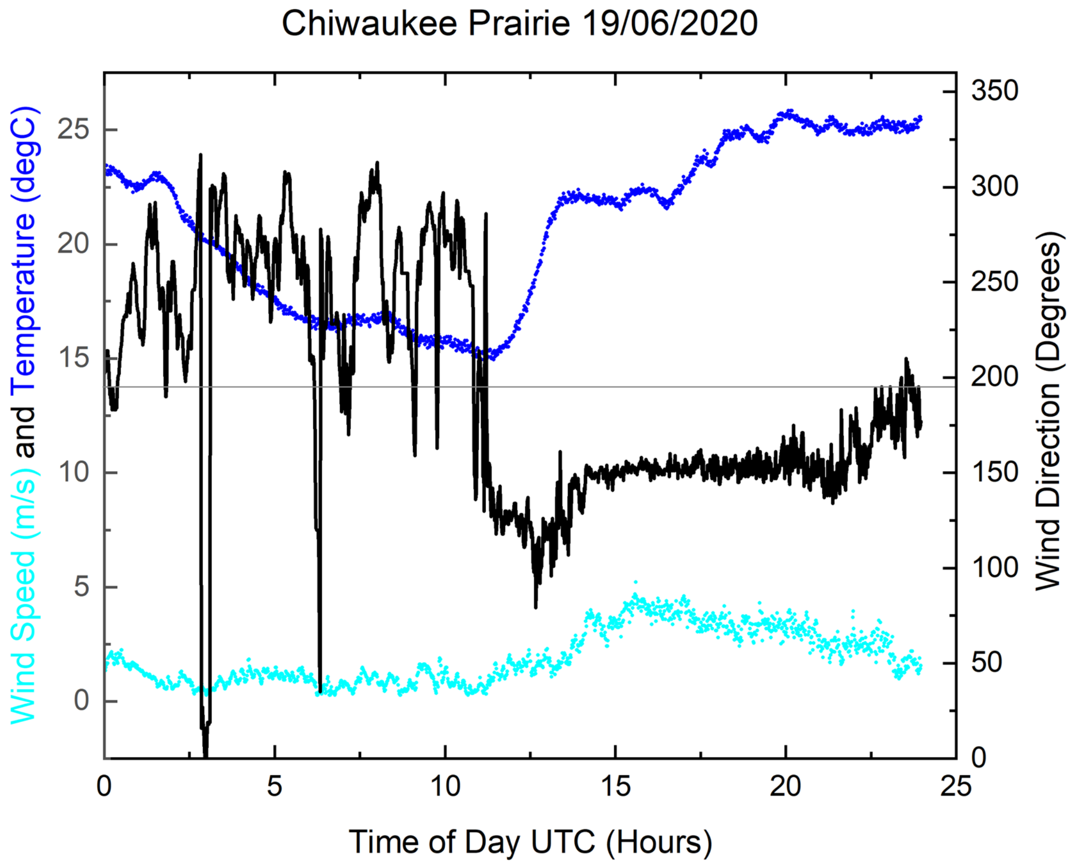

Figure S16: Ground station meteorological observations of wind speed (m/s), direction and air temperature (in ^{o} C) at Chiwaukee Prairie on June 19, 2020

S3. Doppler lidar

A Doppler lidar (Halo Photonics Stream Line XR Doppler lidar) (Pearson et al., 2009) was deployed on the roof of the WDNR Chiwaukee Prairie air monitoring station. The Doppler lidar operated using pulsed near-infrared radiation at a wavelength of 1.5 µm. Doppler lidar observations measured backscatter intensities, wind speeds and directions. The wind profiles were derived from six-point velocity azimuth display (VAD) scans. The depth of the retrieved wind profiles varied significantly from as shallow as 100 m AGL to as deep as 2 km AGL which depend on the presence of scatterers in order to have a detectable signal return.

S3.1 Lidar Wind Pro observations June 15-19:

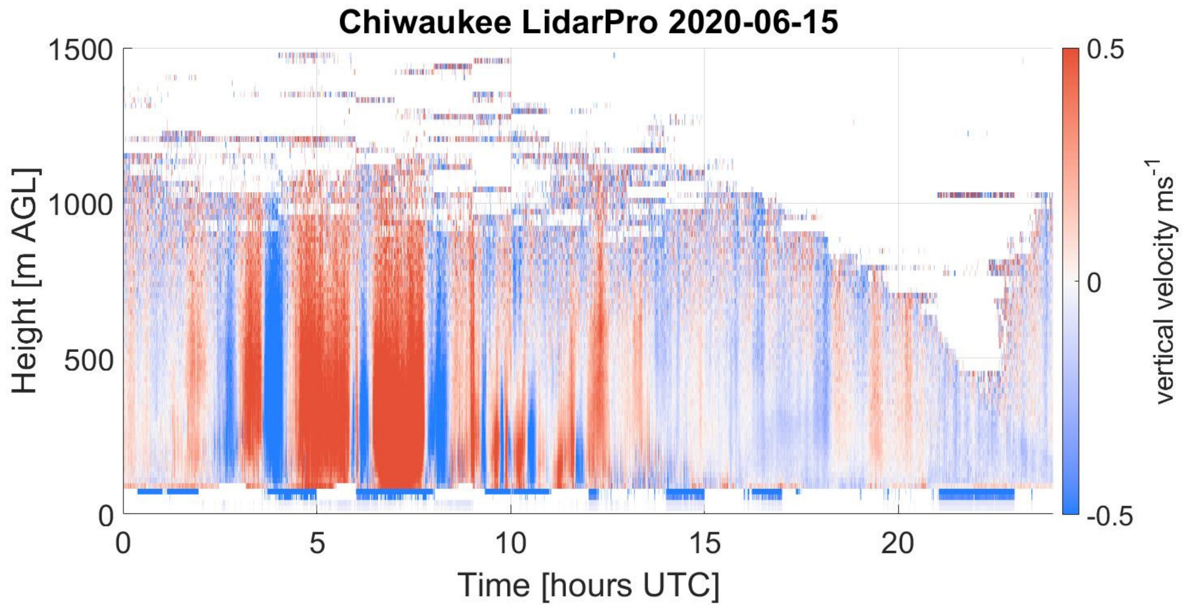

a)

b)

Figure S17: Lidar WindPro observations from.June 15, 2020 with time in UTC a) lidar *u* (zonal) winds (m/s), and b) lidar backscatter.

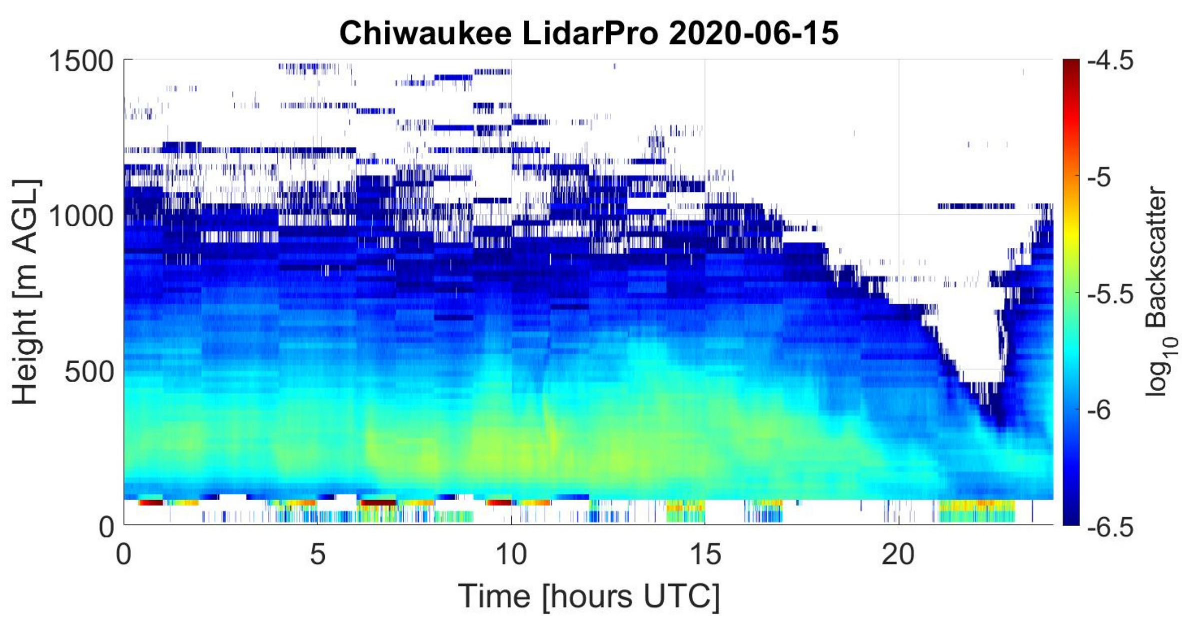

a)

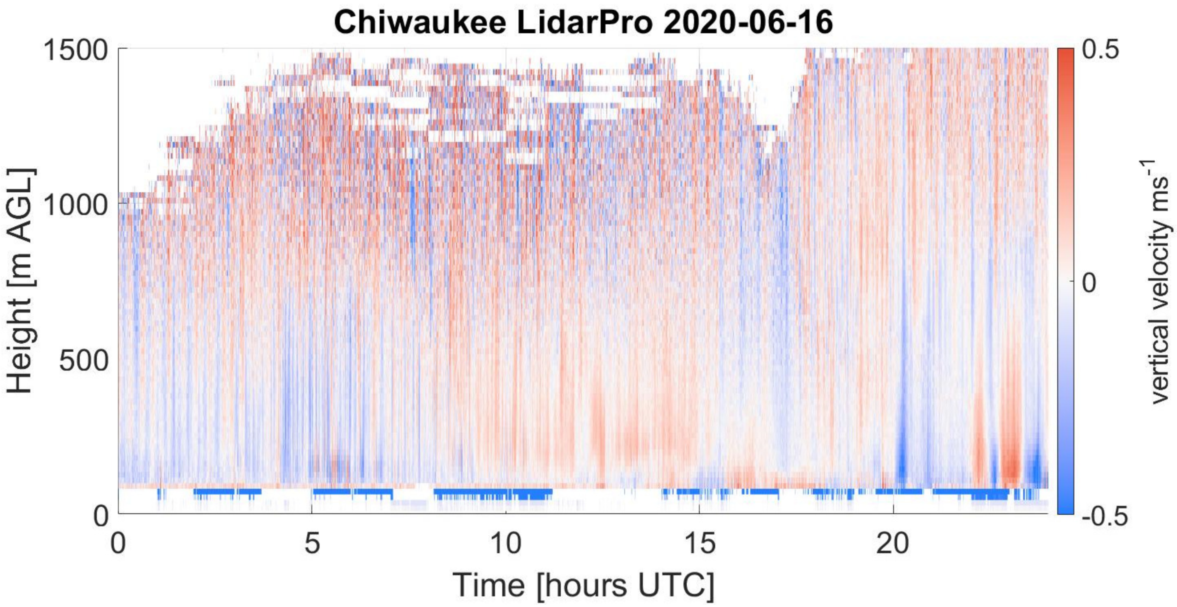

b)

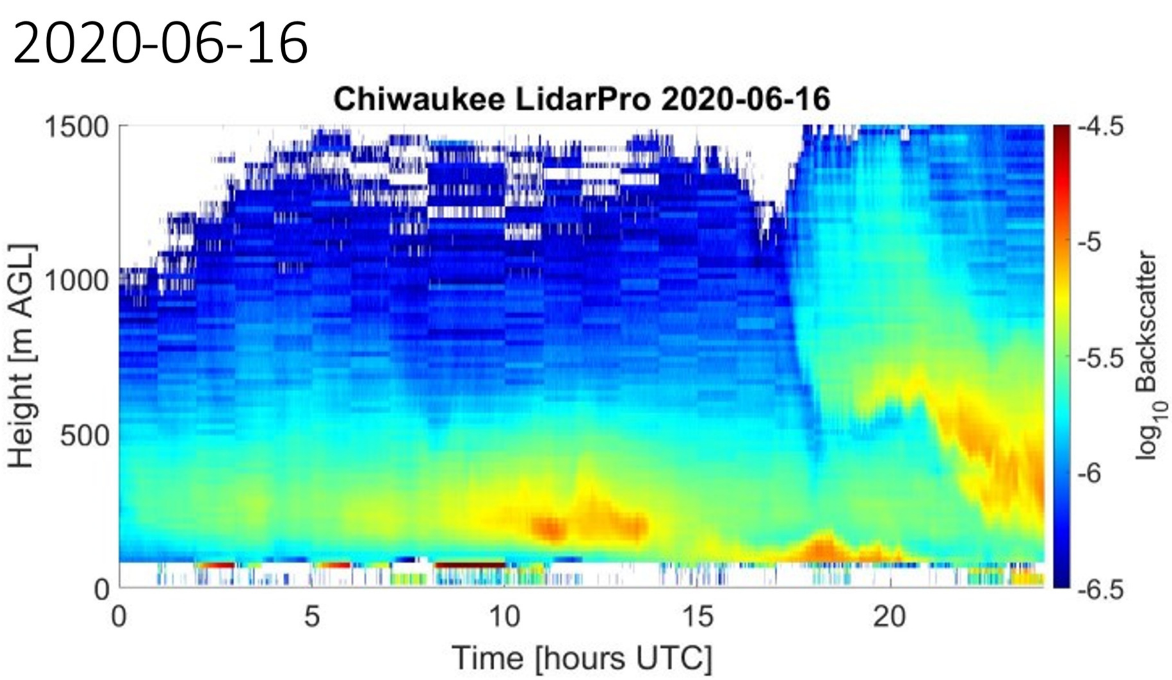

Figure S18 Lidar WindPro observations from June 16 2020 with time in UTC a) lidar *u* (zonal) winds (m/s), and b) lidar backscatter.

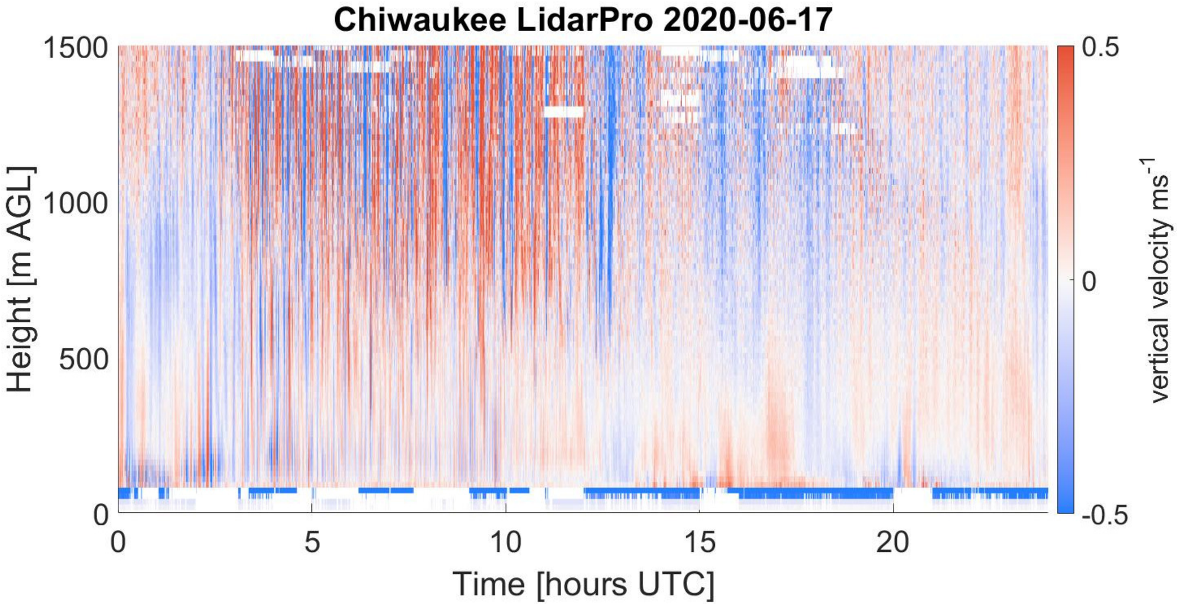

a)

2020-06-17

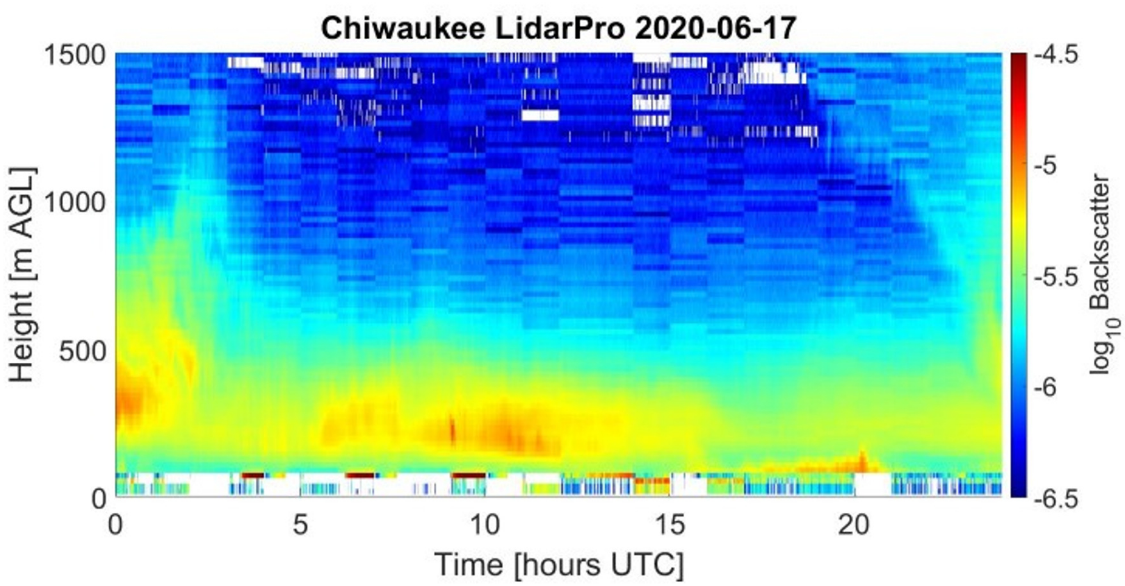

b)

Figure S19 Lidar WindPro observations from June 17, 2020 with time in UTC a) lidar *u* (zonal) winds (m/s), and b) lidar backscatter.

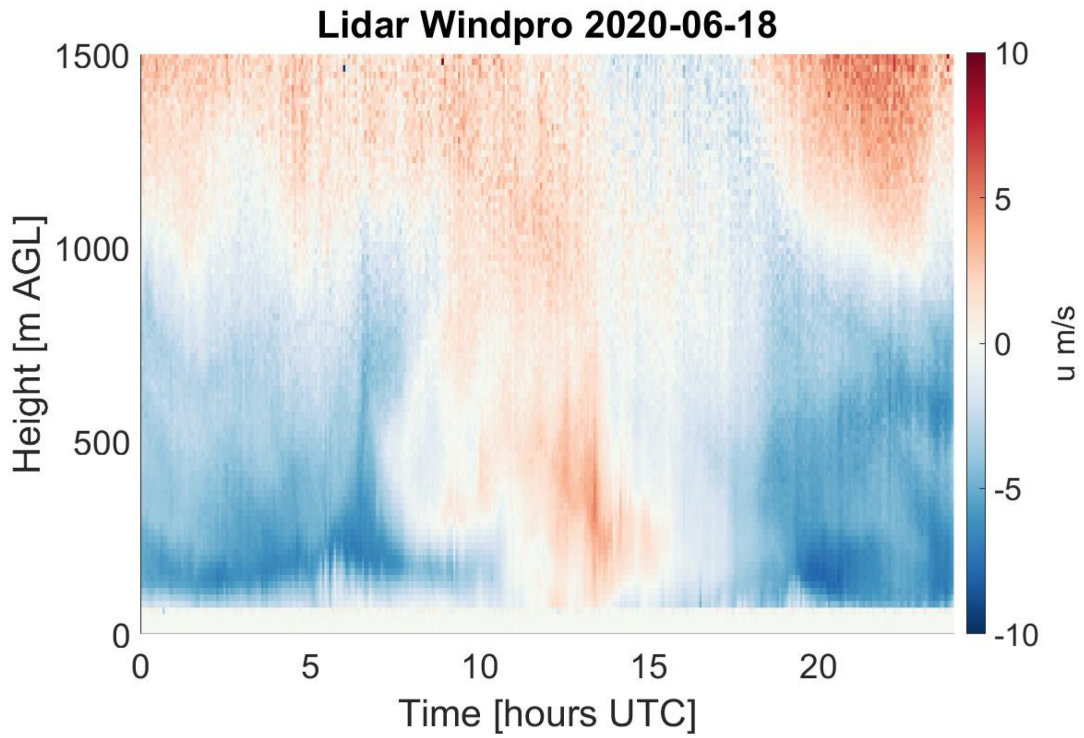

a)

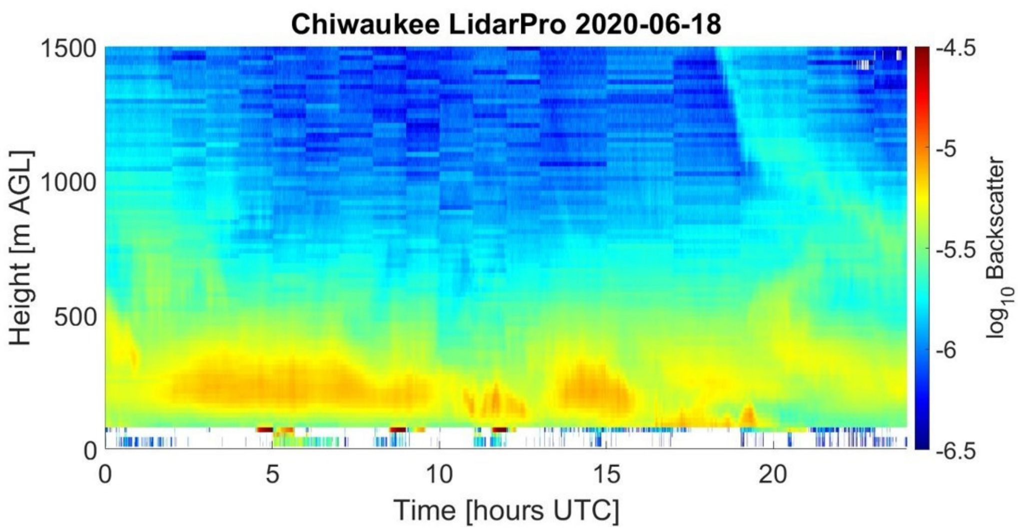

b)

Figure S20 Lidar WindPro observations from.June 18, 2020 with time in UTC a) lidar *u* (zonal) winds (m/s), and b) lidar backscatter.

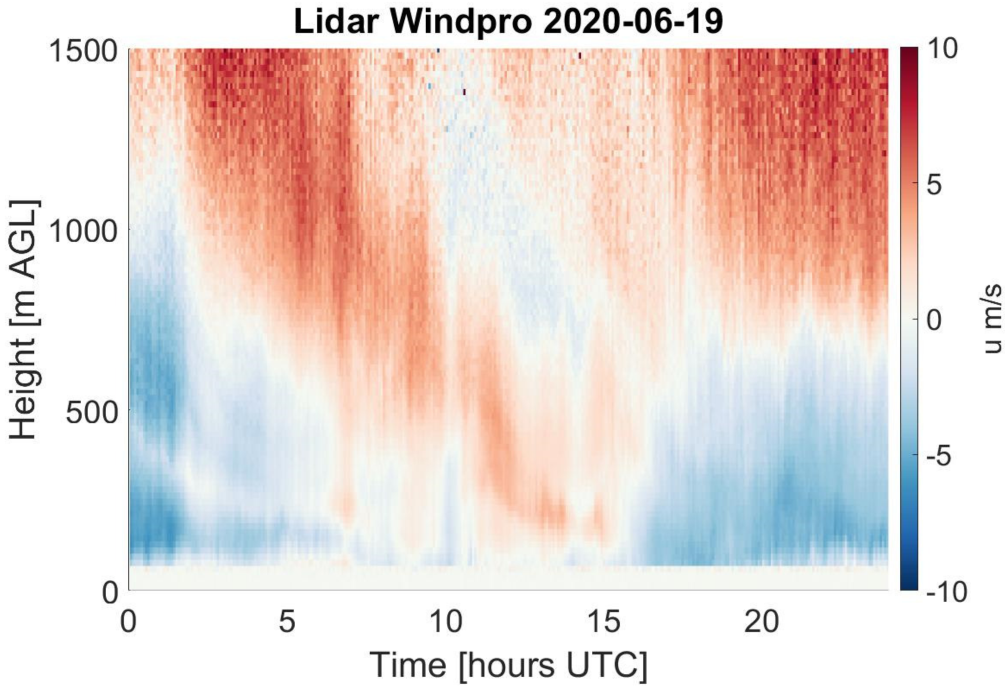

a)

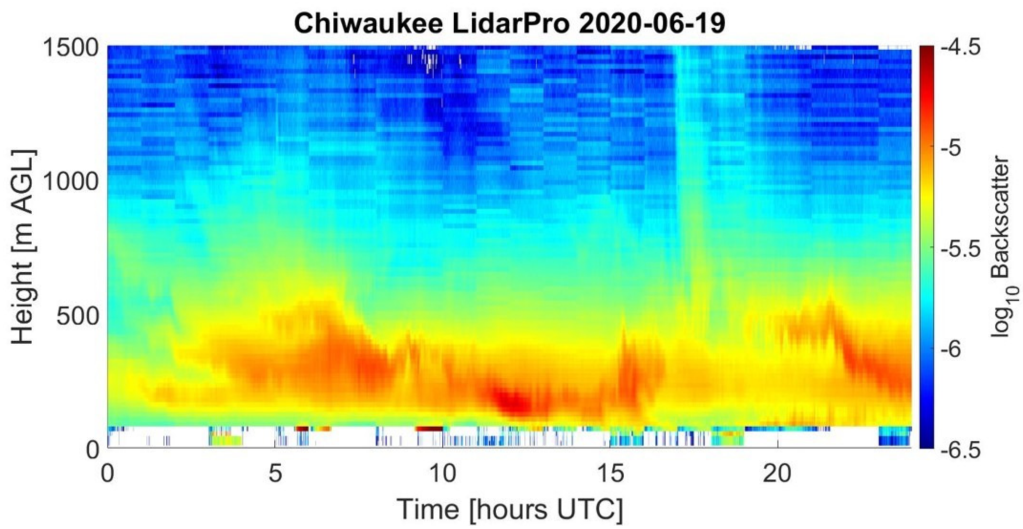

b)

Figure S21: Lidar WindPro observations from June 19, 2020 with time in UTC a) lidar *u* (zonal) winds (m/s), and b) lidar backscatter.

S4. Realtime Air Quality Modeling System, RAQMS

The Realtime Air Quality Modeling System (RAQMS) was utilized in Chiwaukee Prairie during the WISCODisco20 field campaign. RAQMS (Pierce et al., 2003) is a stratospheric and tropospheric chemistry modeling system that was developed by the NASA Langley Research Center and the University of Wisconsin-Madison. RAQMS on-line global chemical predictions account for photochemical and advective processes and the exchange of trace gases through convection and boundary layer turbulence (Pierce et al., 2003). Specifically, for the WISCODisco20 campaign, the RAQMS model with a 1° x 1° latitude-longitude resolution was used for forecasting synoptic scale conditions for deployment during this ozone season.

A comparison with hourly ground observations and 6-hour ozone analyses from the 1° x 1° RAQMS model are given in Figure 4. The resolution of this model is not adequate to capture lake breeze dynamics, particularly if it is shallow. However, the figure illustrates that the RAQMS model generally captures the diurnal and synoptic variation in observed ozone during this period (daytime bias of 11.5 ppbv, nighttime bias of 0.5ppbv, correlation of 0.66 with hourly surface observations), except for June 19, when the RAQMS analysis significantly underestimated ozone concentrations. The disagreement between observations and the model simulation is typical during lake-breeze influenced ozone exceedances, which require much higher (on the order of 1-3km) resolution meteorological and chemical forecasts to predict steep gradients at a shoreline location. Higher resolution modeling efforts would be useful to understand the impact of the marine layer vertical dimensions on the ozone production chemistry.

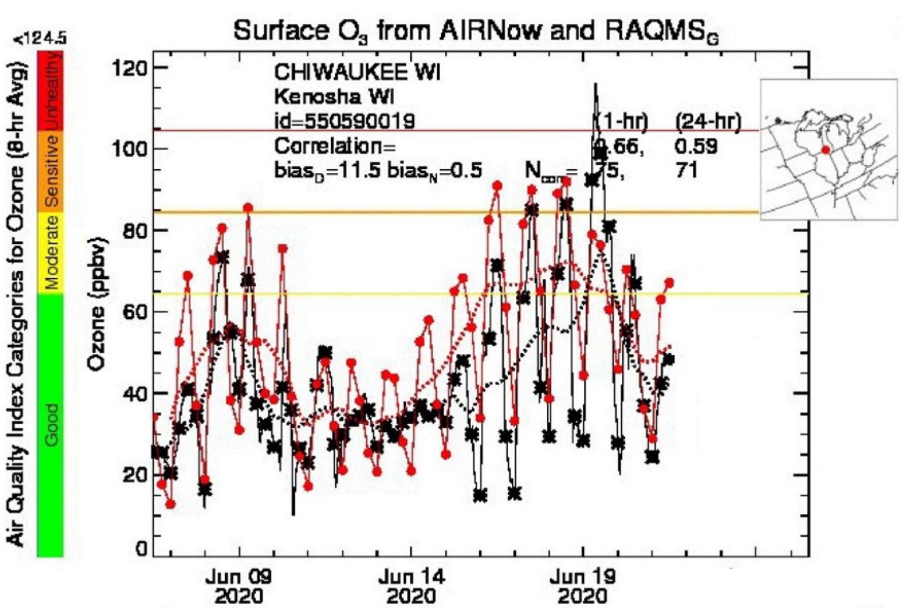

Figure S22: RAQMS instantaneous 8-hour ozone model output at Chiwaukee Prairie (red) and hourly ground station observations (black) from June 7-21, 2020.

Cleary, P. A., Dickens, A., McIlquham, M., Sanchez, M., Geib, K., Hedberg, C., Hupy, J., Watson, M. W., Fuoco, M., Olson, E. R., Pierce, R. B., Stanier, C., Long, R., Valin, L., Conley, S., and Smith, M.: Impacts of lake breeze meteorology on ozone gradient observations along Lake Michigan shorelines in Wisconsin, Atmospheric Environment, 269, 10.1016/j.atmosenv.2021.118834, 2022.
Pearson, G., Davies, F., and Collier, C.: An Analysis of the Performance of the UFAM Pulsed Doppler Lidar for Observing the Boundary Layer, Journal of Atmospheric and Oceanic Technology, 26, 240-250, 10.1175/2008jtecha1128.1, 2009.
Pierce, R. B., Al-Saadi, J. A., Schaack, T., Lenzen, A., Zapotocny, T., Johnson, D., Kittaka, C., Buker, M., Hitchman, M. H., Tripoli, G., Fairlie, T. D., Olson, J. R., Natarajan, M., Crawford, J., Fishman, J., Avery, M., Browell, E. V., Creilson, J., Kondo, Y., and Sandholm, S. T.: Regional Air Quality Modeling System (RAQMS) predictions of the tropospheric ozone budget over east Asia, Journal of Geophysical Research-Atmospheres, 108, 10.1029/2002jd003176, 2003.
Wagner, T. J., Czarnetzki, A. C., Christiansen, M., Pierce, R. B., Stanier, C. O., Dickens, A. F., and Eloranta, E. W.: Observations of the Development and Vertical Structure of the Lake-Breeze Circulation during the 2017 Lake Michigan Ozone Study, Journal of the Atmospheric Sciences, 79, 1005-1020, 10.1175/jas-d-20-0297.1, 2022.